IEEE Access
Multidisciplinary ⋮ Rapid Review ⋮ Open Access Journal

Received February 6, 2018, accepted March 15, 2018, date of publication March 29, 2018, date of current version April 23, 2018.

Digital Object Identifier 10.1109/ACCESS.2018.2820681

Hybrid Tracking Control of 2-DOF SCARA Robot via Port-Controlled Hamiltonian and Backstepping

JIERU CHI, HAISHENG YU, AND JINPENG YU
School of Automation and Electrical Engineering, Qingdao University, Qingdao 266071, China

Corresponding author: Jieru Chi (chijieru@qdu.edu.cn)

This work was supported in part by the National Natural Science Foundation of China under Grant 61573203 and Grant 61573204, in part by the Natural Science Foundation of Shandong Province under Grant ZR2016FM11, and in part by the Science and Technology Project of College and University in Shandong Province under Grant J11LG04.

ABSTRACT In this paper, we propose a hybrid coordinated control method based on port-controlled Hamiltonian and backstepping to improve the position tracking performance for two degree of freedom SCARA robot. The port-controlled Hamiltonian (PCH) control is designated to ensure the stability of the system, and the backstepping control targets to improve the response speed of the system. Exponential function is used as a coordination function to achieve the coordinated control strategy to adapt to the position tracking control of 2-DOF SCARA robot. This hybrid coordination control system not only realizes a quick tracking control, but also improves the steady-state performance of the output signal. The simulation results show that when the external interference exists in the mechanical system of a 2-DOF SCARA robot, the hybrid tracking control system takes on the advantages of both methods, which shows good dynamic performance, good steady-state performance, and strong resistance to external interference.

INDEX TERMS 2-DOF SCARA robot, port-controlled Hamiltonian, backstepping control, position tracking control.

I. INTRODUCTION

Scara robots, known as selective compliance assembly robot arm, have been widely used in the assembly, welding, handling and other industries. Meanwhile, there is an increasing demand for a higher speed and repeatability precision of the SCARA robot [1]. Since the manipulator is a highly nonlinear system, using only one method is difficult to achieve good dynamic and stability performance. The sliding mode surface of sliding mode control is undisturbed by changes of object parameters and the external disturbance, and therefore, the sliding mode control has strong robustness. However, the chattering phenomenon comes with it [3], [4]. Fuzzy control does not need to establish an accurate mathematical model, but its steady-state performance is unsatisfactory [5]. Adaptive control can modify its own characteristics to adapt to the changes in dynamic characteristics and parameters, but the adaptive control theory is not yet integrated, the parameter setting is difficult and the application field is limited [6]. Neural network has powerful capability in nonlinear fitting and precision, but the control algorithm is complicated, and the setting of the network structure and parameters are difficult [7]. The backstepping method can ensures the stability of the whole system by designing the Lyapunov function and inter virtual control variable for each subsystem, until ''back'' to the whole system. The integral links are connected in series to form the whole system control [8]. In recent years, with the development of non-linear control, Port-Controlled Hamiltonian (PCH) has attracted much attention. The Hamiltonian function, the sum of potential energy and kinetic energy in physical systems, is a good candidate of Lyapunov functions for many physical systems. Due to this, the practical control designs and stability analysis of the nonlinear system can be simple [9]–[17]. In our previous study, we found that system using PCH control method could not respond quickly to transient large load changes. To address this drawback, we propose a hybrid control method of PCH and backstepping for the 2-DOF SCARA robot.

The paper is organized as follows. In Section II the kinetic model of the state error PCH systems is briefly given. The PCH controller and backstepping controller design for 2-DOF SCARA robot are detailed in Section III. In Section IV the hybrid control strategy is introduced. Section V reports

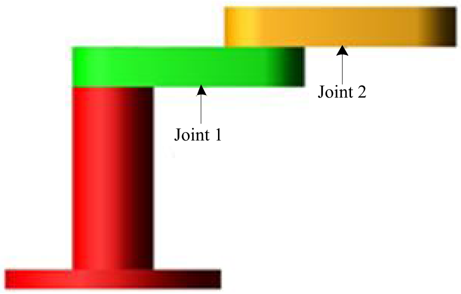

FIGURE 1. The 3D model of 2-DOF SCARA robot.

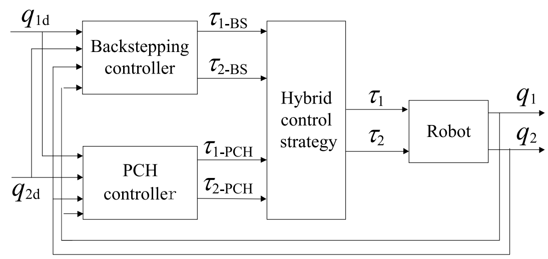

FIGURE 2. The system chart of hybrid control based on PCH and backstepping.

and discusses two descriptive instances, which is followed by the conclusion in Section VI.

II. THE KINETIC MODEL OF 2-DOF SCARA ROBOT

The 3D model of the robot established in ADAMS is shown in Fig. 1.

Then the kinetic model of 2-DOF SCARA robot is deduced based on the D-H coordinate method. The kinetic model can be described by

$$\boldsymbol{\tau} = M(\boldsymbol{q})\ddot{\boldsymbol{q}} + C(\boldsymbol{q}, \dot{\boldsymbol{q}})\dot{\boldsymbol{q}} \tag{1}$$

where $\boldsymbol{\tau}$ is the control torque; $\boldsymbol{q} \in R^2$ is angular displacement vector; $\dot{\boldsymbol{q}} \in R^2$ is angular velocity vector; $\ddot{\boldsymbol{q}} \in R^2$ is angular acceleration vector; $M(\boldsymbol{q}) = \begin{bmatrix} M_{11} & M_{12} \\ M_{21} & M_{22} \end{bmatrix}$ is the inertial matrix; in which $M_{11} = 0.006012 \cos q_2 - 0.00507 \sin q_2 + 0.065$; $M_{12} = M_{21} = 0.003006 \cos q_2 - 0.002535 \sin q_2 + 0.02934$; $M_{22} = 0.02934$; $C(\boldsymbol{q}, \dot{\boldsymbol{q}}) = \begin{bmatrix} C_{11} & C_{12} \\ C_{21} & C_{22} \end{bmatrix}$ is the Coriolis force and centripetal force; in which $C_{11} = (-0.01788 \sin q_2)\dot{q}_2$; $C_{12} = (-0.0008934 \sin q_2)\dot{q}_2$; $C_{21} = (0.0008934 \sin q_2)\dot{q}_1$; $C_{22} = 0$.

III. THE HYBRID CONTROL PRINCIPLE OF 2-DOF SCARA ROBOT

The system chart of hybrid control method based on PCH and backstepping is shown in Fig. 2.

A. DESIGN OF PCH CONTROLLER

1) PCH SYSTEM

The concept of energy dissipation is introduced into the PCH system, and the model of Port-Control Hamiltonian with dissipation (PCHD) can be expressed by

$$\begin{cases} \dot{\boldsymbol{x}} = f(\boldsymbol{x}) + g(\boldsymbol{x})\boldsymbol{\tau_{PCH}} = [J(\boldsymbol{x}) - R(\boldsymbol{x})]\frac{\partial H(\boldsymbol{x})}{\partial \boldsymbol{x}} \\ \qquad + g(\boldsymbol{x})\boldsymbol{\tau_{PCH}} \\ \boldsymbol{y} = h(\boldsymbol{x}) = g^T(\boldsymbol{x})\frac{\partial H(\boldsymbol{x})}{\partial \boldsymbol{x}} \end{cases} \tag{2}$$

where $\boldsymbol{x} \in R^4$ is the state variable, $\boldsymbol{\tau_{PCH}} \in R^2$ is input variable, $\boldsymbol{y} \in R^2$ is output variable, $R(\boldsymbol{x}) = R^T(\boldsymbol{x}) \geq 0$, $J(\boldsymbol{x}) = -J^T(\boldsymbol{x})$. $R(\boldsymbol{x})$ is the semi-positive definite symmetric matrix and it reflects additional resistive structure on the port; $J(\boldsymbol{x})$ is anti-symmetric matrix and it reflects the interconnection structure in the system; $g(\boldsymbol{x})$ reflects the port characteristics of the system.

2) ESTABLISHMENT OF PCH MODEL FOR 2-DOF SCARA ROBOT

Define the state variable and input variable of system as follow

$$\boldsymbol{x} = \begin{bmatrix} \boldsymbol{q} \\ \boldsymbol{p} \end{bmatrix} = \begin{bmatrix} q_1 \\ q_2 \\ p_1 \\ p_2 \end{bmatrix} = \begin{bmatrix} 1 & 0 & 0 & 0 \\ 0 & 1 & 0 & 0 \\ 0 & 0 & M_{11} & M_{12} \\ 0 & 0 & M_{12} & M_{22} \end{bmatrix} \begin{bmatrix} q_1 \\ q_2 \\ \dot{q}_1 \\ \dot{q}_2 \end{bmatrix}$$
$$\boldsymbol{\tau_{PCH}} = \begin{bmatrix} \tau_{1-PCH} & \tau_{2-PCH} \end{bmatrix}^T \tag{3}$$

where $\boldsymbol{q} = [q_1 q_2]^T$ is angular position vector; $\dot{\boldsymbol{q}} = [\dot{q}_1 \dot{q}_2]^T$ is angular velocity vector; $\boldsymbol{p} = \begin{bmatrix} p_1 & p_2 \end{bmatrix}^T = \begin{bmatrix} M_{11} & M_{12} \\ M_{12} & M_{22} \end{bmatrix}\begin{bmatrix} \dot{q}_1 \\ \dot{q}_2 \end{bmatrix}$; $\boldsymbol{\tau_{PCH}} = \begin{bmatrix} \tau_{1-PCH} & \tau_{2-PCH} \end{bmatrix}^T$ is angular control torque.

The PCH system of SCARA robot is the sum of the kinetic and potential energy of the system. Thus the PCH system can be described by

$$H(\boldsymbol{q}, \boldsymbol{p}) = \frac{1}{2}\boldsymbol{p}^T M^{-1}(\boldsymbol{q})\boldsymbol{p} + U(\boldsymbol{q}) \tag{4}$$

From (3) and (4), we can derive the PCH model of 2-DOF SCARA robot, which is shown as

$$\begin{aligned} \dot{\boldsymbol{x}} &= \begin{bmatrix} 0 & 0 & 1 & 0 \\ 0 & 0 & 0 & 1 \\ -1 & 0 & 0 & 0 \\ 0 & -1 & 0 & 0 \end{bmatrix} \begin{bmatrix} 0 \\ C_{12}\dot{q}_1 \\ \dot{q}_1 \\ \dot{q}_2 \end{bmatrix} \\ &\quad + \begin{bmatrix} 0 & 0 \\ 0 & 0 \\ 1 & 0 \\ 0 & 1 \end{bmatrix} \begin{bmatrix} \tau_{1-PCH} \\ \tau_{2-PCH} \end{bmatrix} \\ &= [J(\boldsymbol{x}) - R(\boldsymbol{x})]\frac{\partial H(\boldsymbol{x})}{\partial \boldsymbol{x}} + g(\boldsymbol{x})\boldsymbol{\tau_{PCH}} \\ \boldsymbol{y} &= g^T(\boldsymbol{x})\frac{\partial H(\boldsymbol{x})}{\partial \boldsymbol{x}} = \begin{bmatrix} \dot{q}_1 \\ \dot{q}_2 \end{bmatrix} \end{aligned} \tag{5}$$

where $J(\boldsymbol{x}) = \begin{bmatrix} 0 & I_{2\times 2} \\ -I_{2\times 2} & 0 \end{bmatrix}$, $R(\boldsymbol{x}) = 0$, $g(\boldsymbol{x}) = \begin{bmatrix} 0_{2\times 2} \\ G \end{bmatrix}$, $G = I_{2\times 2}$, $\frac{\partial H(\boldsymbol{x})}{\partial \boldsymbol{x}} = \begin{bmatrix} 0 & C_{12}\dot{q}_1 & \dot{q}_1 & \dot{q}_2 \end{bmatrix}^T$.

The desired balance point of the system is $\boldsymbol{x_d} = \begin{bmatrix} q_{1d} & q_{2d} & p_{1d} & p_{2d} \end{bmatrix}^T = \begin{bmatrix} q_{1d} & q_{2d} & 0 & 0 \end{bmatrix}^T$. In order to stabilize the system asymptotically at the desired balance point of $\boldsymbol{x_d}$, a closed-loop constructed with a feedback control is shown as

$$\dot{\boldsymbol{x}} = [J_d(\boldsymbol{x}) - R_d(\boldsymbol{x})] \frac{\partial H_d(\boldsymbol{x})}{\partial \boldsymbol{x}} \tag{6}$$

where, $H_d(\boldsymbol{x})$ is the desired energy function; $J_d(\boldsymbol{x}) = -J_d^T(\boldsymbol{x})$ is the desired interconnection matrix; $R_d(\boldsymbol{x}) = R_d^T(\boldsymbol{x})$ is the desired resistive matrix.

The expected Hamiltonian function $H_d(\boldsymbol{x})$ is selected as

$$H_d(\boldsymbol{x}) = \frac{1}{2} p^T M_d^{-1} p + \frac{1}{2} q^T K_{P\_PCH} q \tag{7}$$

where $H_d(\boldsymbol{x_d}) = 0$; $M_d = M_d^T = \begin{bmatrix} a_1 & a_2 \\ a_2 & a_3 \end{bmatrix} > 0$ is the desired inertial matrix; $K_{P\_PCH} = diag\left\{K_{P_PCH1} \;\; K_{P_PCH2}\right\} > 0$ is proportional gain.

$J_d(\boldsymbol{x})$ and $R_d(\boldsymbol{x})$ are selected as

$$J_d(\boldsymbol{x}) = \begin{bmatrix} 0 & M^{-1}(\boldsymbol{q}) M_d \\ -M_d M^{-1}(\boldsymbol{q}) & 0 \end{bmatrix}$$
$$R_d(\boldsymbol{x}) = \begin{bmatrix} 0 & 0 \\ 0 & G K_{D\_PCH} G^T \end{bmatrix} \geq 0 \tag{8}$$

where $K_{D\_PCH} = diag\left\{K_{D\_PCH1} \;\; K_{D\_PCH2}\right\} \geq 0$ is differential coefficient.

Comparing Eq. (2) with Eq. (6), one can get

$$g(\boldsymbol{x}) \boldsymbol{\tau_{PCH}} = [J_d(\boldsymbol{x}) - R_d(\boldsymbol{x})] \frac{\partial H_d(\boldsymbol{x})}{\partial \boldsymbol{x}} - [J(\boldsymbol{x}) - R(\boldsymbol{x})] \frac{\partial H(\boldsymbol{x})}{\partial \boldsymbol{x}} \tag{9}$$

Further with the consolidation of Eq. (9), we can get

$$\begin{cases} \tau_{1-PCH} = k_{p11}(q_1 - q_{1d}) + k_{p12}(q_2 - q_{2d}) \\ \qquad + k_{v11}(\dot{q}_1 - \dot{q}_{1d}) + k_{v12}(\dot{q}_2 - \dot{q}_{2d}) \\ \tau_{2-PCH} = k_{p21}(q_1 - q_{1d}) + k_{p22}(q_2 - q_{2d}) \\ \qquad + k_{v21}(\dot{q}_1 - \dot{q}_{1d}) + k_{v22}(\dot{q}_2 - \dot{q}_{2d}) \\ \qquad + C_{12}\left(\dot{q}_1^2 + \dot{q}_1 \dot{q}_2\right) \end{cases} \tag{10}$$

where

$$\begin{aligned} k_{p11} &= \frac{K_{P_PCH1}}{|M(\boldsymbol{q})|}(a_2 M_{12} - a_1 M_{22}), \\ k_{p12} &= \frac{K_{P_PCH2}}{|M(\boldsymbol{q})|}(a_1 M_{12} - a_2 M_{11}), \\ k_{v11} &= \frac{K_{D\_PCH1}}{|M_d|}(a_2 M_{12} - a_3 M_{11}), \\ k_{v12} &= \frac{K_{D\_PCH1}}{|M_d|}(a_2 M_{22} - a_3 M_{12}), \\ k_{p21} &= \frac{K_{P\_PCH1}}{|M(\boldsymbol{q})|}(a_3 M_{12} - a_2 M_{22}), \\ k_{p22} &= \frac{K_{P\_PCH2}}{|M(\boldsymbol{q})|}(a_2 M_{12} - a_3 M_{11}), \\ k_{v21} &= \frac{K_{D\_PCH2}}{|M_d|}(a_2 M_{11} - a_1 M_{12}), \\ k_{v22} &= \frac{K_{D\_PCH2}}{|M_d|}(a_2 M_{12} - a_1 M_{22}). \end{aligned}$$

B. THE STABILITY ANALYSIS OF PCH CONTROL SYSTEM

Define the desired function of Hamiltonian of PCH system is

$$V_{PCH} = H_d(\boldsymbol{x}) = \frac{1}{2} \boldsymbol{p}^T M_d^{-1} \boldsymbol{p} + \frac{1}{2} \boldsymbol{q}^T K_{P\_PCH} \boldsymbol{q} \tag{11}$$

It is obvious that $V_{PCH} = H_d(\boldsymbol{x}) > 0$. From Eq. (8), we can obtain $J_d(\boldsymbol{x})$ is anti-symmetric matrix and $R_d(\boldsymbol{x})$ is positive semi-definite matrix. Then $\dot{V}_{PCH}$ is computed by

$$\begin{aligned} \dot{V}_{PCH} &= \frac{\partial H_d(\boldsymbol{x})}{\partial t} = \left[\frac{\partial H_d(\boldsymbol{x})}{\partial \boldsymbol{x}}\right]^T \dot{\boldsymbol{x}} \\ &= \left[\frac{\partial H_d(\boldsymbol{x})}{\partial \boldsymbol{x}}\right]^T \left[[J_d(\boldsymbol{x}) - R_d(\boldsymbol{x})] \frac{\partial H_d(\boldsymbol{x})}{\partial \boldsymbol{x}}\right] \\ &= -\left[\frac{\partial H_d(\boldsymbol{x})}{\partial \boldsymbol{x}}\right]^T R_d(\boldsymbol{x}) \left[\frac{\partial H_d(\boldsymbol{x})}{\partial \boldsymbol{x}}\right] \leq 0 \end{aligned} \tag{12}$$

According to LaSalle's invariant set theory, if the closed loop control system is part of the set of

$$\left\{ \boldsymbol{x} \in R^n \left| \left[\frac{\partial H_d(\boldsymbol{x})}{\partial \boldsymbol{x}}\right]^T R_d(\boldsymbol{x}) \frac{\partial H_d(\boldsymbol{x})}{\partial \boldsymbol{x}} = 0 \right. \right\}$$

and the maximum set in it is 0, then the PCH subsystem is asymptotically stable at the point of $\boldsymbol{x_d}$.

C. DESIGN OF BACKSTEPPING CONTROLLER

Define $\boldsymbol{x_1} = \boldsymbol{q}$ and $\boldsymbol{x_2} = \dot{\boldsymbol{q}}$. To facilitate the procedure of backstepping controller, the kinetic model (1) can be written as the following form

$$\begin{cases} \dot{\boldsymbol{x}}_1 = \boldsymbol{x_2} \\ \dot{\boldsymbol{x}}_2 = M^{-1}(\boldsymbol{q}) \boldsymbol{\tau_{BS}} - M^{-1}(\boldsymbol{q}) C(\boldsymbol{q}, \dot{q}) \boldsymbol{x_2} \\ \boldsymbol{y} = \boldsymbol{x_1} \end{cases} \tag{13}$$

where $\boldsymbol{\tau_{BS}} = \begin{bmatrix} \tau_{1-BS} & \tau_{2-BS} \end{bmatrix}^T$ is angular control torque of beckstepping controller.

Define the desired output of the control system as $\boldsymbol{y_d} = [q_{1d} q_{2d}]^T$.

Step1: Define the tracking error variable and its first derivative,

$$\begin{aligned} \boldsymbol{e_1} &= \boldsymbol{y} - \boldsymbol{y_d} = [q_1 - q_{1d} \quad q_2 - q_{2d}]^T \\ \dot{\boldsymbol{e}}_1 &= \dot{\boldsymbol{x}}_1 - \dot{\boldsymbol{y}}_d = \boldsymbol{x_2} - \dot{\boldsymbol{y}}_d \end{aligned} \tag{14}$$

Choose the first Lyapunov function

$$V_1 = \frac{1}{2} \boldsymbol{e_1^T e_1} \tag{15}$$

The time derivative of V_1 is computed by

$$\dot{V}_1 = \boldsymbol{e_1^T} \dot{\boldsymbol{e}}_1 = \boldsymbol{e_1^T}(\boldsymbol{x_2} - \dot{\boldsymbol{y}}_d) \tag{16}$$

To guarantee negativity of the first Lyapunov function derivative, a desired virtual controller is selected

$$\boldsymbol{x_{2d}} = -K_1 \boldsymbol{e_1} + \dot{\boldsymbol{y}}_d \tag{17}$$

where $K_1 = diag\left\{k_1^1 \;\; k_1^2\right\}$, k_1^1 and k_1^2 are the positive constant.

To stabilize the first subsystem, let $\boldsymbol{x_2} = \boldsymbol{x_{2d}}$, and substitute Eq. (17) into Eq. (16). We can get $\dot{V}_1 = -\boldsymbol{e_1^T} K_1 \boldsymbol{e_1} \leq 0$.

Step 2: Choose the virtual control error vector of the second subsystem as $\boldsymbol{e_2} = \boldsymbol{x_2} - \boldsymbol{x_{2d}}$, and then $\dot{e}_2$ can be calculated by

$$\dot{\boldsymbol{e}}_2 = M^{-1}(\boldsymbol{q})\boldsymbol{\tau_{BS}} - M^{-1}(\boldsymbol{q})C(\boldsymbol{q}, \dot{\boldsymbol{q}})\boldsymbol{x_2} - \dot{\boldsymbol{x}}_{2d} \tag{18}$$

The second Lyapunov function V_2 is defined as

$$V_2 = V_1 + \frac{1}{2}\boldsymbol{e}_2^T\boldsymbol{e_2} = \frac{1}{2}\boldsymbol{e}_1^T\boldsymbol{e_1} + \frac{1}{2}\boldsymbol{e}_2^T\boldsymbol{e_2} \tag{19}$$

Obviously, $\dot{V}_2$ can be computed as

$$\begin{aligned}\dot{V}_2 &= \boldsymbol{e}_1^T\dot{\boldsymbol{e}}_1 + \boldsymbol{e}_2^T\dot{\boldsymbol{e}}_2 \\ &= -\boldsymbol{e}_1^T K_1 \boldsymbol{e_1} \\ &\quad + \boldsymbol{e}_2^T \left(M^{-1}(\boldsymbol{q})\,\boldsymbol{\tau_{BS}} - M^{-1}(\boldsymbol{q})\,C(\boldsymbol{q}, \dot{\boldsymbol{q}})\,\boldsymbol{x_2} - \dot{\boldsymbol{x}}_{2d}\right)\end{aligned} \tag{20}$$

To guarantee $\dot{V}_2 < 0$, construct the control law τ_{BS} as

$$\boldsymbol{\tau_{BS}} = M(\boldsymbol{q})\left(-K_2\boldsymbol{e_2} + M^{-1}(\boldsymbol{q})\,C(\boldsymbol{q}, \dot{\boldsymbol{q}})\,\boldsymbol{x_2} + \dot{\boldsymbol{x}}_{2d}\right) \tag{21}$$

where $K_2 = diag\left\{k_2^1\ k_2^2\right\}$, k_2^1 and k_2^2 are the positive constant.
Then, employing Eq. (21), Eq. (20) becomes

$$\dot{V}_2 = -\boldsymbol{e}_1^T K_1 \boldsymbol{e_1} - \boldsymbol{e}_2^T K_2 \boldsymbol{e_2} < 0 \tag{22}$$

Further with the consolidation of Eq. (21), the control law τ_{BS} can be rewritten as

$$\begin{cases}\tau_{1_{BS}} = k_{b11}q_1 + k_{b12}q_2 + k_{s11}\dot{q}_1 + k_{s12}\dot{q}_2 + b_1 \\ \tau_{2_{BS}} = k_{b21}q_1 + k_{b22}q_2 + k_{s21}\dot{q}_1 + k_{s22}\dot{q}_2 + b_2\end{cases} \tag{23}$$

where $k_{b11} = -M_{11}k_2^1k_1^1$, $k_{b12} = -M_{12}k_2^2k_1^2$,

$$\begin{aligned}k_{s11} &= \left(C_{11} - M_{11}k_2^1 - M_{11}k_1^1\right), \\ k_{s12} &= \left(C_{12} - M_{12}k_2^2 - M_{12}k_1^2\right), \\ b_1 &= M_{11}k_2^1k_1^1q_{1d} + M_{12}k_2^2k_1^2q_{2d}, \\ k_{b21} &= -M_{21}k_2^1k_1^1,\ k_{b22} = -M_{22}k_2^2k_1^2k_1^2, \\ k_{s21} &= \left(C_{21} - M_{21}k_2^1 - M_{21}k_1^1\right), \\ k_{s22} &= \left(-M_{22}k_2^2 - M_{22}k_1^2\right), \\ b_2 &= M_{21}k_2^1k_1^1q_{1d} + M_{22}k_2^2k_1^2q_{2d}.\end{aligned}$$

D. THE STABILITY ANALYSIS of BACKSTEPPING CONTROL SYSTEM

Define Lyapunov function of backstepping control system as

$$V_{BS} = V_2 = \frac{1}{2}\boldsymbol{e}_1^T\boldsymbol{e_1} + \frac{1}{2}\boldsymbol{e}_2^T\boldsymbol{e_2} \tag{24}$$

On the condition Obviously, V_{BS} is positive definite. In addition, from Eq. (22), we can know that $\dot{V}_{BS}$ is negative semi-definite. According the Lyapunov stability theory, the backstepping control system is asymptotically stable.

IV. DESIGN OF HYBRID COMTROL STRATEGY BASED ON PCH AND BACKSTEPPING

Since PCH control and backstepping control are complementary with each other, the hybrid control strategy designed in this paper can make full use of advantages of two control methods in the corresponding time. The hybrid control system has good performance of dynamic and steady-state, and the ability to resist interference is improved.

A. DESIGN OF HYBRID CONTROL STRATEGY

Definec_{1-PCH}, c_{2-PCH} as the coordinated functions of PCH controller; Define c_{1-BS}, c_{2-BS} as the coordinated functions of backstepping controller. Assume the start time is t_1, $|q - q_d| > \beta\ rad/s$ (β is constant, $\beta > 0$). Then the coordinated functions can be designed as

$$\begin{cases}c_{1-PCH}(t) = 1 - e^{-(t-t_1)/T_C}, & c_{1-BS}(t) = e^{-(t-t_1)/T_C} \\ c_{2-PCH}(t) = 1 - e^{-(t-t_1)/T_C}, & c_{2-BS}(t) = e^{-(t-t_1)/T_C}\end{cases} \tag{25}$$

where T_C is coordinated time, $c_{1-PCH} \in [0, 1]$, $c_{2-PCH} \in [0, 1]$, $c_{1-BS} \in [0, 1]$, $c_{1-BS} \in [0, 1]$.
Then we can get the hybrid control strategy

$$\begin{cases}\tau_1 = c_{1-PCH}(t)\tau_{1-PCH} + c_{1-BS}(t)\tau_{1-BS} \\ \tau_2 = c_{2-PCH}(t)\tau_{2-PCH} + c_{2-BS}(t)\tau_{2-BS}\end{cases} \tag{26}$$

B. THE STABILITY ANALYSIS OF ROBOT TRAJECTORY TRACKING CONTROL SYSTEM BASED on PCH AND BACKSTEPPING

Define the Lyapunov function of the whole system to be

$$V = V_{BS} + V_{PCH} \tag{27}$$

On the condition that $t = t_1$, $c_{1-PCH}(t) = c_{2-PCH}(t) = 0$, $c_{1-BS}(t) = c_{2-BS}(t) = 1$. This means that only the backstepping controller plays a role on the system. We have $V = V_{BS} > 0$, $\dot{V} = \dot{V}_{BS} \leq 0$, and so the system is stable.

On the condition that $t_1 < t < \infty$, the coordinated functions are all constants between 0 and 1. As the time increases, the intensity of backstepping controller is gradually reduced, and the intensity of PCH controller is gradually increased. Since there is no change on the type of the two controllers, so the Lyapunov function of the whole system is $V = V_{BS} + V_{PCH}$, then $\dot{V} = \dot{V}_{BS} + \dot{V}_{PCH}$. According to the stability analysis of the backstepping control system and PCH control system, we can get the result that V_{BS} and V_{PCH} are positive definite, $\dot{V}_{BS}$ and $\dot{V}_{PCH}$ are negative semi-definite, so V is positive definite and $\dot{V}$ is negative semi-definite. Therefore the whole system is asymptotically stable.

On the condition that $t \to \infty$, $c_{1-PCH}(t) = c_{2-PCH}(t) = 1$, $c_{1-BS}(t) = c_{2-BS}(t) = 0$. This means that only the PCH controller plays a role on the system. We have $V = V_{PCH} > 0$, $\dot{V} = \dot{V}_{PCH} \leq 0$, and so the system is stable.

We can conclude that the control system is asymptotically stable based on the analysis above.

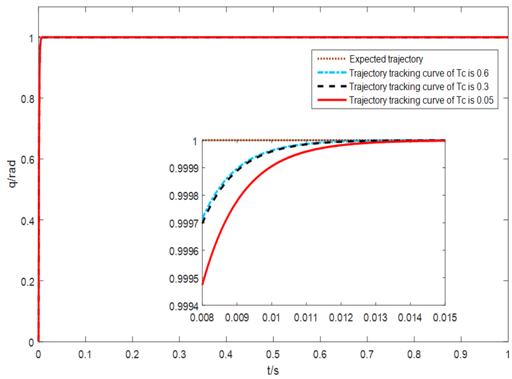

FIGURE 3. Curves with different coordinated time of joint 1.

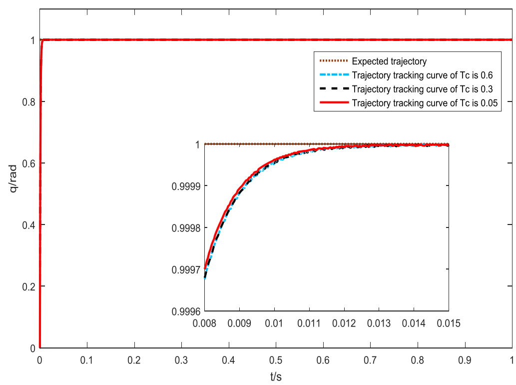

FIGURE 4. Curves with different coordinated time of joint 2.

V. THE SIMULATION AND ANALYSIS

In order to verify the control performance of the hybrid control method, a tracking control system of 2-DOF SCARA robot based on PCH and backstepping is established in MATLAB/Simulink. Parameters of the simulation used as shown in the following.

Parameters of PCH controller: $K_{P_PCH1} = 200000$, $K_{P_PCH2} = 20000$, $K_{D\_PCH1} = 10000$, $K_{D_PCH2} = 1$, $a_1 = 0.05$, $a_2 = 0.0001$, $a_3 = 0.0001$. Parameters of backstepping controller: $k_1^1 = k_1^2 = 1000$, $k_2^1 = k_2^2 = 200000$. The start time of the hybrid controller: $t_1 = 0.0001s$. In order to compare and observe, the initial displacement and the velocity are zero.

A. SIMULATION OF UNIT STEP SIGNALS

The expected position signals of joint 1and joint 2 are unit step signals. Fig. 3 and Fig. 4 are the trajectory curves of joint 1 and joint 2 at different coordinated times. According to Fig. 3 and Fig. 4, the coordinated time are $T_{C1} = 0.05$, $T_{C2} = 0.3$, $T_{C3} = 0.6$. In order to make joint 1 and joint 2 both have faster response speed and better control effect, $T_{C1} = 0.3$ is chosen as the coordinated time at the simulation experiment of the hybrid control.

Fig. 5 and Fig. 6 are the trajectory curves of different control methods for joint 1 and joint 2. According to Fig. 5 and Fig. 6, the backstepping control has faster response speed, but has a small amount of steady-state errors; the PCH control has good performance of steady-state, but the response speed is lower than backstepping control; and the hybrid control has good performance in terms of both response speed and steady-state.

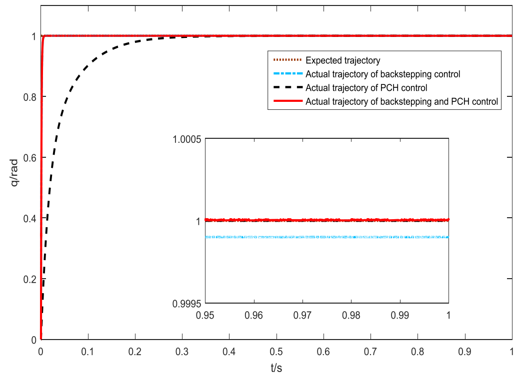

FIGURE 5. Curves with different control methods of joint 1.

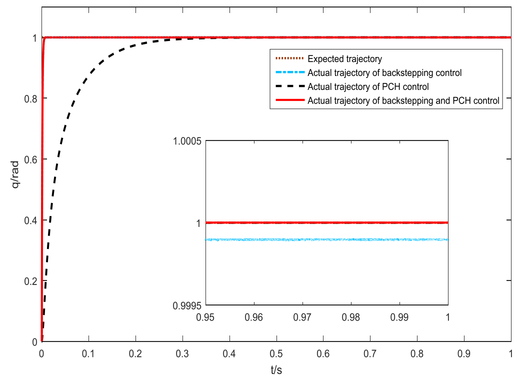

FIGURE 6. Curves with different control methods of joint 2.

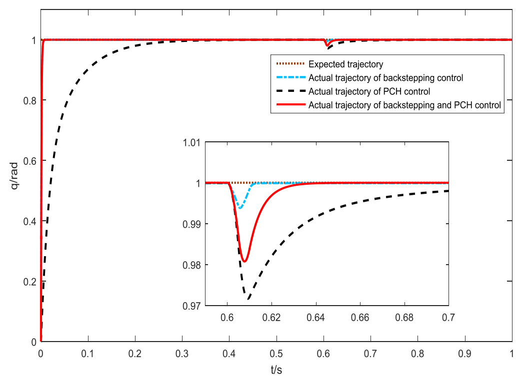

FIGURE 7. Curves with effect of interference of joint 1.

Fig. 7 and Fig. 8 are the trajectory curves when there is a disturbance imposed at the time of $t = 0.6s$. According to Fig. 7 and Fig. 8, the waveform of backstepping control has small changes which reflects the backstepping has strong ability to resist interference; the waveform of PCH control system changes greatly which reflects PCH control has poor performance to resist interference; and the waveform of hybrid control changes smaller compared with PCH control which reflects the ability to resist interference improved.

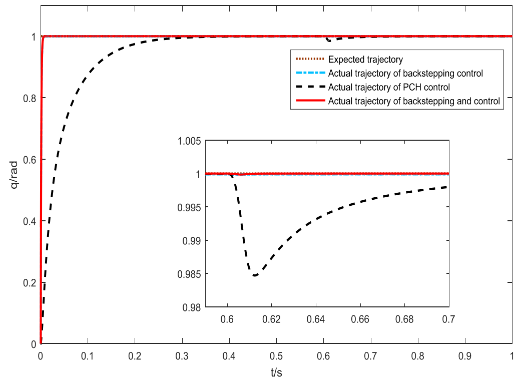

FIGURE 8. Curves with effect of interference of joint 2.

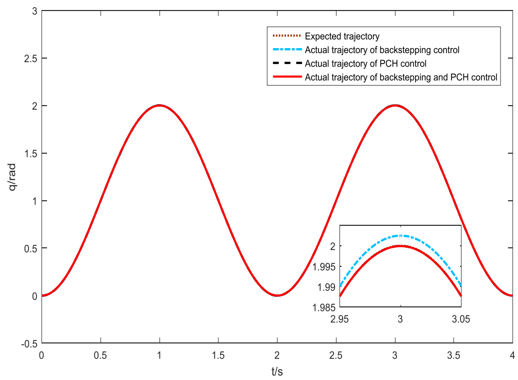

FIGURE 9. Curves with different control methods of joint 1.

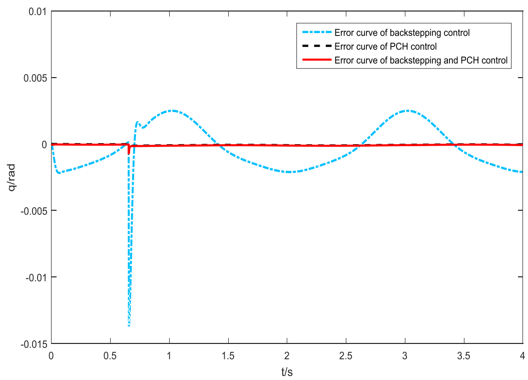

FIGURE 10. Error curves with different control methods of joint 1.

Remark 1: From the simulations, it can be clearly seen that the hybrid control method based on PCH and backstepping has good dynamic performance and steady-state performance, and the ability to resist the interference is improved. It is easily observed that the backstepping control is used to improve the response speed in the initial moment, and PCH control is used to improve the steady-state in steady state.

B. SIMULATION OF CONTINUOUS TRAJECTORY TRACKING CONTROL

In order to compare and observe, a simple motion planning is designed: the expected large arm trajectory is

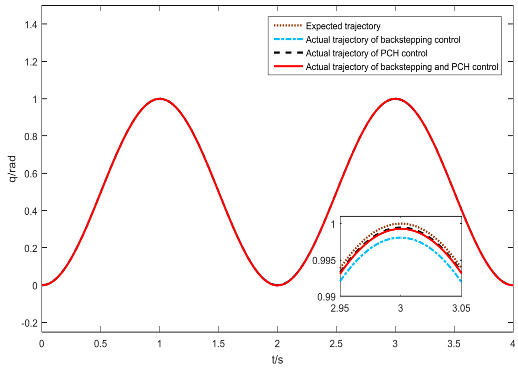

FIGURE 11. Curves with different control methods of joint 2.

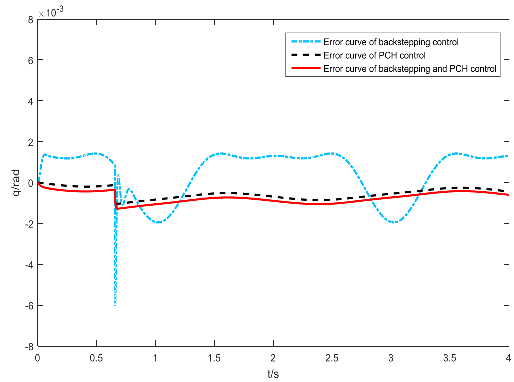

FIGURE 12. Error curves with different control methods of joint 2.

$q_{1d} = 1 - \cos(\pi t)$, and the expected small arm trajectory is $q_{2d} = 0.5 - 0.5\cos(\pi t)$. The planning trajectory is consistent with the displacement, velocity and acceleration constraints of the robot. There is no external interference.

Fig. 9 and Fig. 10 are the trajectory curves and error curves of different control methods for joint 1. As shown in Fig. 9 and Fig. 10, for the joint 1, the trajectory tracking curves with different control methods are very good, except that there is a small amount of steady-state errors in the backstepping control method.

Fig. 11 and Fig. 12 are the trajectory curves and error curves of different control methods for joint 2. According to Fig. 11 and Fig. 12, for the joint 2, the trajectory tracking curves produced by hybrid control and PCH control are very close, but there is a certain error between the curve of backstepping control and the other curves.

Remark 2: By comparison, the hybrid control can effectively combine the advantages of backstepping control and PCH control at the corresponding time. The hybrid control system has good performance on dynamic and steady-state, which mean that the proposed method in this paper is more suitable for practical engineering.

VI. CONCLUSION

In this paper, a hybrid control method based on PCH and backstepping is designed for 2-DOF SCARA robot position tracking control. Backstepping control is used to improve the response speed in the initial moment, and PCH control is used to improve the steady-state in steady state. The hybrid control strategy proposed in this paper can make the advantages of each method be fully utilized at the corresponding time, and the change in the control form greatly increases its practical value. The simulation results show that the hybrid control of PCH and backstepping has good dynamic performance and steady-state performance, and the ability to resist the interference is improved.

In practical applications, the load torque of joint is usually unknown. In order to track the changes of the load torque better and eliminate steady error, the control torque observer would be designed in the future. In addition, in order to make the research more valuable, we will increase the freedom of the robot and use the servo motor as the driving mechanism in the future work.

REFERENCES

[1] S. M. Ahmadi and M. M. Fateh, "Robust control of electrically driven robots using adaptive uncertainty estimation," *Comput. Elect. Eng.*, vol. 56, pp. 674–687, Nov. 2016.

[2] F. G. Rossomando and C. M. Soria, "Adaptive neural sliding mode control in discrete time for a SCARA robot arm," *IEEE Latin Amer. Trans.*, vol. 14, no. 6, pp. 2556–2564, Jun. 2016.

[3] C. Urrea and J. Kern, "Trajectory tracking control of a real redundant manipulator of the SCARA type," *J. Elect. Eng. Technol.*, vol. 11, no. 1, pp. 215–226, Jan. 2016.

[4] M. Pourrahim, K. Shojaei, A. Chatraei, and O. S. Nazari, "Experimental evaluation of a saturated output feedback controller using RBF neural networks for SCARA robot IBM 7547," in *Proc. Iran. Conf. Elect. Eng. (ICEE)*, May 2016, pp. 1347–1352.

[5] M. M. Fateh and S. Fateh, "A precise robust fuzzy control of robots using voltage control strategy," *Int. J. Autom. Comput.*, vol. 10, no. 1, pp. 64–72, Feb. 2013.

[6] T. Benjanarasuth, N. Sowannee, and N. Naksuk, "Two-degree-of-freedom simple servo adaptive control for SCARA robot," in *Proc. Int. Conf. Control, Autom. Syst. (ICCAS)*, Oct. 2010, pp. 480–484.

[7] M. A. Al-Khedher and M. S. Alshamasin, "SCARA robot control using neural networks," in *Proc. Int. Conf. Intell. Adv. Syst. (ICIAS)*, vol. 1. Jun. 2012, pp. 126–130.

[8] N. Nikdel, M. A. Badamchizadeh, V. Azimirad, and M. A. Nazari, "Adaptive backstepping control for an n-degree of freedom robotic manipulator based on combined state augmentation," *Robot. Comput.-Integr. Manuf.*, vol. 44, pp. 129–143, Apr. 2017.

[9] Q. Zhang and G. Liu, "Precise control of elastic joint robot using an interconnection and damping assignment passivity-based approach," *IEEE/ASME Trans. Mechatron.*, vol. 21, no. 6, pp. 2728–2736, Dec. 2016.

[10] Q. Zhang, Z. Xie, S. Kui, H. Yang, J. Minghe, and H. Cai, "Interconnection and damping assignment passivity-based control for flexible joint robot," in *Proc. World Congr. Intell. Control Autom. (WCICA)*, Mar. 2015, pp. 4242–4249.

[11] S. El-Ferik, A. Qureshi, and F. L. Lewis, "Robust neuro-adaptive cooperative control of multi-agent port-controlled Hamiltonian systems," *Int. J. Adapt. Control Signal Process.*, vol. 30, no. 3, pp. 488–510, Mar. 2015.

[12] A. Qureshi, S. El Ferik, and F. L. Lewis, "L_2 neuro-adaptive tracking control of uncertain port-controlled Hamiltonian systems," *IET Control Theory Appl.*, vol. 9, no. 12, pp. 1781–1790, Aug. 2015.

[13] K. Nunna, M. Sassano, and A. Astolfi, "Constructive interconnection and damping assignment for port-controlled hamiltonian systems," *IEEE Trans. Autom. Control*, vol. 60, no. 9, pp. 2350–2361, Sep. 2015.

[14] A. Sanz and V. Etxebarria, "Interconnection and damping assignment passivity-based experimental control of a single-link flexible robot arm," in *Proc. IEEE Int. Conf. Control Appl.*, Oct. 2007, pp. 2504–2509.

[15] P. Staufer and H. Gattringer, "Passivity-based tracking control of a flexible link robot," in *Multibody Syst. Dynam., Robot., Control*, pp. 95–112, Jan. 2013.

[16] D. Jeltsema, R. Ortega, and J. M. A. Scherpen, "An energy-balancing perspective of interconnection and damping assignment control of nonlinear systems," *Automatica*, vol. 40, no. 9, pp. 1643–1646, Sep. 2004.

[17] R. Ortega, A. J. van der Schaft, B. M. Maschke, and G. Escobar, "Interconnection and damping assignment passivity-based control of port-controlled Hamiltonian systems," *Automatica*, vol. 38, no. 4, pp. 585–596, Apr. 2002.

JIERU CHI received the B.Sc. degree in automation and M.Sc. degree in control science and engineering from Shandong University, Jinan, China, in 1992 and 1995, respectively. She is currently pursuing the Ph.D. degree at the Institute of Complexity Science, Qingdao University, Qingdao, China. She is currently an Associate Professor with the School of Automation and Electrical Engineering, Qingdao University. Her current research interests include motor control and robot control, applied nonlinear control, and intelligent systems.

HAISHENG YU received the B.S. degree in electrical automation from the Harbin University of Civil Engineering and Architecture, Harbin, China, in 1985, the M.S. degree in computer applications from Tsinghua University, Beijing, China, in 1988, and the Ph.D. degree in control science and engineering from Shandong University, Jinan, China, in 2006. He is currently a Professor with the School of Automation and Electrical Engineering, Qingdao University, Qingdao, China. His research interests include electrical energy conversion and motor control, applied nonlinear control, computer control, and intelligent systems.

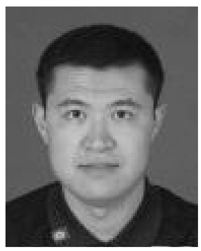

JINPENG YU received the B.Sc. degree in automation from Qingdao University, Qingdao, China, in 2002, the M.Sc. degree in system engineering from Shandong University, Jinan, China, in 2006, and the Ph.D. degree from the Institute of Complexity Science, Qingdao University, in 2011. He is currently a Distinguished Professor with the School of Automation and Electrical Engineering, Qingdao University. His current research interests include electrical energy conversion and motor control, applied nonlinear control, and intelligent systems. He was a recipient of the Shandong Province Taishan Scholar Special Project Fund and the Shandong Province Fund for Outstanding Young Scholars.